

Two-Particle Schrödinger Equation Animations of Wavepacket–Wavepacket Scattering (revised)

Jon J.V. Maestri*, Rubin H. Landau†
Oregon State University
Department of Physics
Corvallis, OR 97331

Manuel J. Páez
Department of Physics
University of Antioquia
Medellin, Colombia

November 26, 2024

Abstract

A simple and explicit technique for the numerical solution of the two-particle, time-dependent Schrödinger equation is assembled and tested. The technique can handle interparticle potentials that are arbitrary functions of the coordinates of each particle, arbitrary initial and boundary conditions, and multi-dimensional equations. Plots and animations are given here and on the World Wide Web of the scattering of two wavepackets in one dimension

1 Introduction

Rather than showing the time dependence of two particles interacting with each other, quantum mechanics textbooks often present a time-independent view of a single particle interacting with an external potential. In part, this makes the physics clearer, and in part, this reflects the difficulty of solving the time-independent two-particle Schrödinger equation for the motion of wavepackets. In the classic quantum mechanics text by Schiff [1], examples of realistic quantum scattering, such as that in Fig. 1, are produced by computer simulations of wave packets colliding with square potential barriers and wells. Generations of students have carried memories of these images (or of the film loops containing these frames [2]) as to what realistic quantum scattering looks like.

While Fig. 1 is a good visualization of a quantum scattering processes, we wish to extend simulations of realistic quantum interactions to include particle–particle scattering when both particles are represented by wavepackets. Although more complicated, this, presumably, is closer to nature and may illustrate some physics not usually found in quantum mechanics textbooks. In addition, our extension goes beyond the treatment found in most computational physics texts which concentrate on *one-particle* wavepackets [3, 4, 5], or highly restricted forms of *two-particle* wavepackets [6].

The simulations of the time-dependent Schrödinger equation shown by Schiff were based on the 1967 finite-difference algorithms developed by Goldberg *et al.* [2]. Those simulations, while revealing, had problems with stability and probability conservation. A decade later,

*Present address: CH2M Hill, P.O.Box 428, Corvallis, OR 97330

†rubin@physics.orst.edu, <http://www.physics.orst.edu/~rubin>

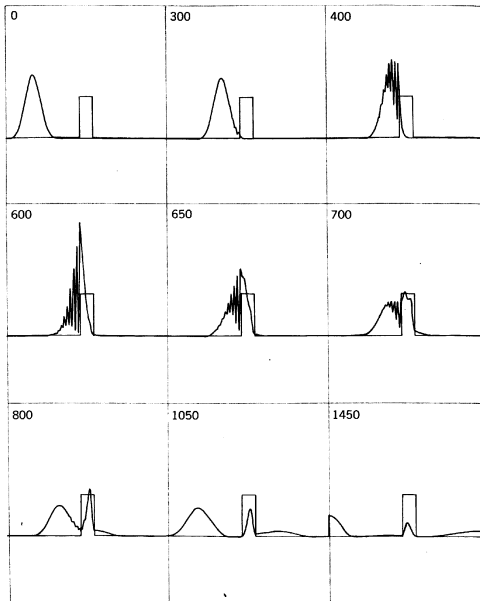


Figure 1: A time sequence of a Gaussian wavepacket scattering from a square barrier as taken from the textbook by Schiff. The mean energy equals the barrier height.

Cakmak and Askar [7] solved the stability problem by using a better approximation for the time derivative. After yet another decade, Visscher [8] solved the probability conservation problem by solving for the real and imaginary parts of the wave function at slightly different (“staggered”) times.

In this paper we combine the advances of the last 20 years and extend them to the numerical solution of the *two particle*—in contrast to the *one particle*—time-dependent Schrödinger equation. Other than being independent of spin, no assumptions are made regarding the functional form of the interaction or initial conditions, and, in particular, there is no requirement of separation into relative and center-of-mass variables[6]. The method is simple, explicit, robust, easy to modify, memory preserving, and may have research applications. However, high precision does require small time and space steps, and, consequently, long running times. A similar approach for the time-dependent one-particle Schrödinger equation in a two-dimensional space has also been studied [5].

2 Two-Particle Schrödinger Equation

We solve the two-particle time-dependent Schrödinger equation

$$i\frac{\partial}{\partial t}\psi(x_1, x_2, t) = H\psi(x_1, x_2, t), \quad (1)$$

$$H = -\frac{1}{2m_1}\frac{\partial^2}{\partial x_1^2} - \frac{1}{2m_2}\frac{\partial^2}{\partial x_2^2} + V(x_1, x_2). \quad (2)$$

where, for simplicity, we assume a one-dimensional space and set $\hbar = 1$. Here H is the Hamiltonian operator and m_i and x_i are the mass and position of particle $i = 1, 2$. Knowledge of the two-particle wave function $\psi(x_1, x_2, t)$ permits the calculation of the probability

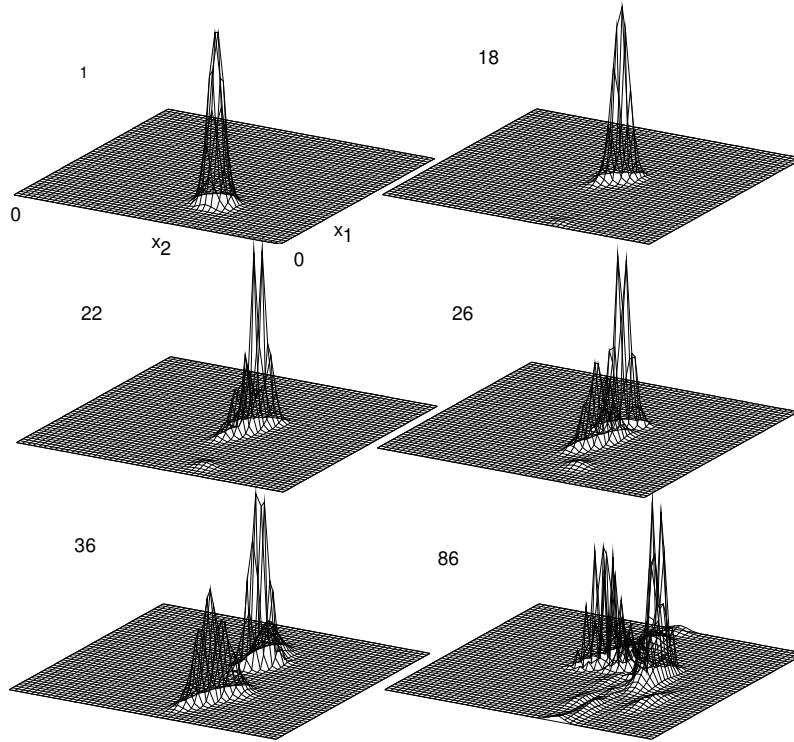


Figure 2: Six frames from an animation of the two-particle density $\rho(x_1, x_2, t)$ as a function of the particle positions x_1 and x_2 , for a repulsive m - $10m$ collision in which the mean kinetic energy equals twice the barrier height. The numbers in the left hand corners give the times in units of $100\Delta t$.

density for particle 1 being at x_1 and particle 2 being at x_2 at time t :

$$\rho(x_1, x_2, t) = |\psi(x_1, x_2, t)|^2. \quad (3)$$

The fact that particles 1 and 2 must be located someplace in space leads to the normalization constraint on the wave function:

$$\int_{-\infty}^{+\infty} \int_{-\infty}^{+\infty} dx_1 dx_2 |\psi(x_1, x_2, t)|^2 = 1. \quad (4)$$

The description of a single particle within a multi-particle system by a single-particle wave function is an approximation unless the system is uncorrelated (in which case the total wave function can be written in product form). However, it is possible to deduce meaningful one-particle densities from the two-particle density by integrating over the other particle:

$$\rho_1(x_i, t) = \int_{-\infty}^{+\infty} dx_j \rho(x_1, x_2, t), \quad (i \neq j = 1, 2). \quad (5)$$

Here we use a subscript on the single-particle density ρ_i to distinguish it from the two-particle density ρ . Of course, the true solution is $\psi(x_1, x_2, t)$, but we find it hard to see the physics in a three-variable complex function, and so, often, view $\rho_1(x_1, t)$ and $\rho_2(x_2, t)$ as two separate wavepackets colliding.

If particles 1 and 2 are identical, then their total wave function should be symmetric or antisymmetric under interchange of the particles. We impose this condition on our numerical solution $\psi(x_1, x_2)$, by forming the combinations

$$\psi'(x_1, x_2) = \frac{1}{\sqrt{2}} [\psi(x_1, x_2) \pm \psi(x_2, x_1)] \quad \Rightarrow \quad (6)$$

$$2\rho(x_1, x_2) = |\psi(x_1, x_2)|^2 + |\psi(x_2, x_1)|^2 \pm 2\text{Re} [\psi^*(x_1, x_2)\psi(x_2, x_1)]. \quad (7)$$

The cross term in (7) places an additional correlation into the wavepackets.

3 Numerical Method

We solve the two-particle Schrödinger equation (1) via a finite difference method that converts the partial differential equation into a set of simultaneous, algebraic equations. First, we evaluate the dependent variable ψ on a grid of discrete values for the independent variables [2]:

$$\psi(x_1, x_2, t) = \psi(x_1 = l\Delta x_1, x_2 = m\Delta x_2, t = n\Delta t) \equiv \psi_{l,m}^n, \quad (8)$$

where l , m , and n are integers. The space part of the algorithm is based on Taylor expansions of $\psi(x_1, x_2, t)$ in *both* the x_1 and x_2 variables up to $\mathcal{O}(\Delta x^4)$; for example,

$$\frac{\partial^2 \psi}{\partial x_1^2} \simeq \frac{\psi(x_1 + \Delta x_1, x_2) - 2\psi(x_1, x_2) + \psi(x_1 - \Delta x_1, x_2)}{\Delta x_1^2} + \mathcal{O}(\Delta x_1^2). \quad (9)$$

In discrete notation, the RHS of the Schrödinger equation (1) now becomes:

$$H\psi = -\frac{\psi_{l+1,m} - 2\psi_{l,m} + \psi_{l-1,m}}{2m_1\Delta x_1^2} - \frac{\psi_{l,m+1} - 2\psi_{l,m} + \psi_{l,m-1}}{2m_2\Delta x_2^2} + V_{l,m}\psi_{l,m}. \quad (10)$$

Next, we express the time derivative in (1) in terms of finite time differences by taking the formal solution to the time-dependent Schrödinger equation and making a forward-difference approximation for time evolution operator:

$$\psi_{l,m}^{n+1} = e^{-i\Delta t H} \psi_{l,m}^n \simeq (1 - i\Delta t H) \psi_{l,m}^n. \quad (11)$$

Although simple, this approximation scheme is unstable since the term multiplying ψ has eigenvalue $(1 - iE\Delta t)$ and modulus $\sqrt{1 + E^2\Delta t^2}$, and this means the modulus of the wave function increases with each time step [3]. The improvement introduced by Askar and Cakmak [7] is a central difference algorithm also based on the formal solution (11):

$$\psi_{l,m}^{n+1} - \psi_{l,m}^{n-1} = (e^{-i\Delta t H} - e^{i\Delta t H}) \psi_{l,m}^n \simeq -2i\Delta t H \psi_{l,m}^n, \quad (12)$$

$$\begin{aligned} \Rightarrow \quad \psi_{l,m}^{n+1} &\simeq \psi_{l,m}^{n-1} - 2i \left[\left\{ \left(\frac{1}{m_1} + \frac{1}{m_2} \right) 4\lambda + \Delta x V_{l,m} \right\} \psi_{l,m}^n \right. \\ &\quad \left. - \lambda \left\{ \frac{1}{m_1} (\psi_{l+l,m}^n + \psi_{l-1,m}^n) + \frac{1}{m_2} (\psi_{l,m+1}^n + \psi_{l,m-1}^n) \right\} \right], \end{aligned} \quad (13)$$

where we have assumed $\Delta x_1 = \Delta x_2$ and formed the ratio $\lambda = \Delta t / \Delta x^2$.

Equation (13) is an *explicit* solution in which the wave function at only two past time values must be stored simultaneously in memory to determine all future times by continued iteration. In contrast, an *implicit* solution determines the wave function for all future times

in just one step, yet this one step requires the solution of simultaneous algebraic equations involving all space and time values. Accordingly, an implicit solution requires the inversion of exceedingly large ($\sim 10^{10} \times 10^{10}$) matrices.

While the explicit method (13) produces a solution which is stable and second-order accurate in time, in practice, it does not conserve probability well. Visscher[8] has deduced an improvement which takes advantage of the extra degree of freedom provided by the complexity of the wave function to preserve probability better. If we separate the wave function into real and imaginary parts,

$$\psi_{l,m}^{n+1} = u_{l,m}^{n+1} + i v_{l,m}^{n+1}, \quad (14)$$

the algorithm (13) separates into the pair of coupled equations:

$$u_{l,m}^{n+1} = u_{l,m}^{n-1} + 2 \left[\left\{ \left(\frac{1}{m_1} + \frac{1}{m_2} \right) 4\lambda + \Delta t V_{l,m} \right\} v_{l,m}^n - \lambda \left\{ \frac{1}{m_1} (v_{l+1,m}^n + v_{l-1,m}^n) + \frac{1}{m_2} (v_{l,m+1}^n + v_{l,m-1}^n) \right\} \right], \quad (15)$$

$$v_{l,m}^{n+1} = v_{l,m}^{n-1} - 2 \left[\left\{ \left(\frac{1}{m_1} + \frac{1}{m_2} \right) 4\lambda + \Delta t V_{l,m} \right\} u_{l,m}^n - \lambda \left\{ \frac{1}{m_1} (u_{l+1,m}^n + u_{l-1,m}^n) + \frac{1}{m_2} (u_{l,m+1}^n + u_{l,m-1}^n) \right\} \right]. \quad (16)$$

Visscher's advance evaluates the real and imaginary parts of the wave function at slightly different (staggered) times,

$$[u_{l,m}^n, v_{l,m}^n] = [\text{Re } \psi(x, t), \text{Im } \psi(x, t + \frac{1}{2}\Delta t)], \quad (17)$$

and uses a definition for probability density that differs for integer and half-integer time steps,

$$\rho(x, t) = |\text{Re } \psi(x, t)|^2 + \text{Im } \psi(x, t + \frac{\Delta t}{2}) \text{Im } \psi(x, t - \frac{\Delta t}{2}), \quad (18)$$

$$\rho(x, t + \frac{\Delta t}{2}) = \text{Re } \psi(x, t + \Delta t) \text{Re } \psi(x, t) + \left| \text{Im } \psi(x, t + \frac{\Delta t}{2}) \right|^2. \quad (19)$$

These definitions reduce to the standard one for infinitesimal Δt , and provide an algebraic cancellation of errors so that probability is conserved.

4 Simulations

We assume that the particle-particle potential is central and depends only on the relative distance between particles 1 and 2 (the method can handle any x_1 and x_2 functional dependences). We have investigated a "soft" potential with a Gaussian dependence, and a "hard" one with a square-well dependence, both with range α and depth V_0 :

$$V(x_1, x_2) = \begin{cases} V_0 \exp[-\frac{|x_1 - x_2|^2}{2\alpha^2}] & \text{(Gaussian)} \\ V_0 \theta(\alpha - |x_1 - x_2|) & \text{(Square)} \end{cases}. \quad (20)$$

Parameter	Value
Δx	0.001
Δt	2.5×10^{-7}
k_1	+157
k_2	-157
σ	0.05
x_1^0	467 (0.33×1401 steps)
x_2^0	934 (0.667×1401 steps)
$N_1 = N_2$	1399
L	1.401 (1401 space steps)
T	0.005 (20,000 time steps)
V_0	-100,000
α	0.062

Table 1: Table 1, Parameters for the antisymmetrized, m-m collision with an attractive square well potential.

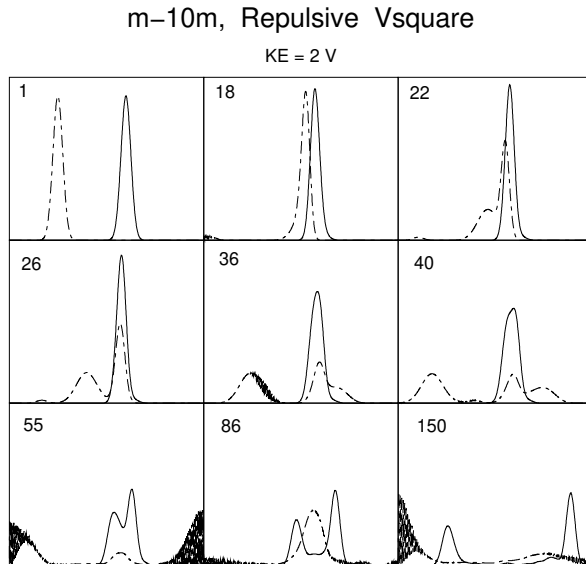


Figure 3: A time sequence of two Gaussian single-particle wavepackets scattering from each other under the influence of a square barrier. The mean energy equals twice the barrier height. The dashed curve describes a particle of mass m and the solid curve one of mass $10m$. The number in the upper left-hand corner of each frame is the time in units of $100\Delta t$, and the edges of the frames correspond to the walls of the box.

4.1 Initial and Boundary Conditions

We model a scattering experiment in which particle 1, initially at x_1^0 with momentum k_1 , collides with particle 2, initially far away at x_2^0 with momentum k_2 , by assuming a product of independent wavepackets for particles 1 and 2:

$$\psi(x_1, x_2, t = 0) = e^{ik_1x_1} \exp\left[-\frac{(x_1 - x_1^0)^2}{4\sigma^2}\right] \times e^{ik_2x_2} \exp\left[-\frac{(x_2 - x_2^0)^2}{4\sigma^2}\right]. \quad (21)$$

Because of these Gaussian factors, ψ is not an eigenstate of the particle i momentum operators $-i\partial/\partial x_i$, but instead contains a spread of momenta about the mean, initial momenta k_1 and k_2 . If the wavepacket is made very broad ($\sigma \rightarrow \infty$), we would obtain momentum eigenstates. Note, that while the Schrödinger equation may separate into one equation in the relative coordinate x and another in the center-of-mass coordinate X , the initial condition (21), or more general ones, cannot be written as separate conditions on x and X . Accordingly, a solution of the equation in each particle coordinate is required [6].

We start the staggered-time algorithm with the real part the wave function (21) at $t = 0$ and the imaginary part at $t = \Delta t/2$. The initial imaginary part follows by assuming that $\Delta t/2$ is small enough, and σ large enough, for the initial time dependence of the wavepacket to be that of the plane wave parts:

$$\begin{aligned} \text{Im} \psi(x_1, x_2, t = \frac{\Delta t}{2}) &\simeq \sin \left[k_1 x_1 + k_2 x_2 - \left(\frac{k_1^2}{2m_1} + \frac{k_2^2}{2m_2} \right) \frac{\Delta t}{2} \right] \\ &\times \exp \left[-\frac{(x_1 - x_1^0)^2 + (x_2 - x_2^0)^2}{2\sigma^2} \right]. \end{aligned} \quad (22)$$

In a scattering experiment, the projectile enters from infinity and the scattered particles are observed at infinity. We model that by solving our partial differential equation within a box of side L (ideally) much larger than both the range of the potential and the width of the initial wavepacket. This leads to the boundary conditions

$$\psi(0, x_2, t) = \psi(x_1, 0, t) = \psi(L, x_2, t) = \psi(x_1, L, t) = 0. \quad (23)$$

The largeness of the box minimizes the effects of the boundary conditions during the collision of the wavepackets, although at large times there will be interesting, yet artificial, collisions with the box.

Some typical parameters used in our tests are given in Table 1 (the code with sample files are available on the on Web [9]). Our space step size $\Delta x = 0.001$ is 1/1,400th of the size of the box L , and 1/70th of the size ($\sqrt{2}\sigma \simeq 0.07$) of the wavepacket. Our time step $\Delta t = 2.5 \times 10^{-7}$ is 1/20,000th of the total time T , and 1/2,000th of a typical time for the wavepacket $[2\pi/(k_1^2/2m_1) \simeq 5 \times 10^{-4}]$. In all cases, the potential and wavepacket parameters are chosen to be similar to those used in the one-particle studies by Goldberg *et al.*. The time and space step sizes were determined by trial and error until values were found which provided stability and precision (too large a Δx leads to spurious ripples during interactions). In general, stability is obtained by making Δt small enough [8], with simultaneous changes in Δt and Δx made to keep $\lambda = \Delta t/\Delta x^2$ constant. Total probability, as determined by a double Simpson's-rule integration of (4), is typically conserved to 13 decimal places, impressively close to machine precision. In contrast, the mean energy, for which we do not use a definition optimized to staggered times, is conserved only to 3 places.

m=10m, Attractive Vsquare

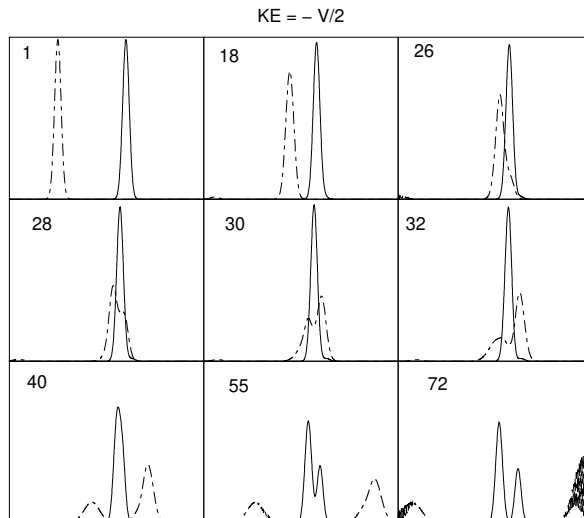


Figure 4: Same as Fig. 3 except now the potential is attractive with the mean energy equal to half the depth.

4.2 Barrier-Like Collisions

We solve our problem in the center-of-momentum system by taking $k_2 = -k_1$ (particle 1 moving to larger x values and particle 2 to smaller x). Our first simulations and Web animations [9] emulate the one-particle collisions with barriers and wells studied by Goldberg *et al.* and presented by Schiff. We make particle 2 ten times heavier than particle 1, so that particle 2’s initial wavepacket moves at 1/10th the speed of particle 1’s, and so looks like a barrier. Although we shall describe several scattering events, the animations available on the Web speak for themselves, and we recommend their viewing.

In Fig. 2 we show six frames from an animation of the two-particle density $\rho(x_1, x_2, t)$ as a simultaneous function of the particle positions x_1 and x_2 . In Fig. 3 we show, for this same collision, the *single-particle* densities $\rho_1(x = x_1, t)$ and $\rho_2(x = x_2, t)$ extracted from $\rho(x_1, x_2, t)$ by integrating out the dependence on the other particle via (5). Since the mean energy equals twice the maximum height of the potential barrier, we expect complete penetration of the packets, and indeed, at time 18 we see that the wavepackets have large overlap, with the repulsive interaction “squeezing” particle 2 (it gets narrower and taller). During times 22–40 we see part of wavepacket 1 reflecting off wavepacket 2 and then moving back to smaller x (the left). From times 26–55 we also see that a major part of wavepacket 1 gets “trapped” inside of wavepacket 2 and then leaks out rather slowly.

We see that for times 1–26, the x_2 position of the peak of $\rho(x_1, x_2, t)$ in Fig. 2 changes very little with time, which is to be expected since particle 2 is heavy. In contrast, the x_1 dependence in $\rho(x_1, x_2, t)$ gets broader with time, develops into two peaks at time 26, separates into two distinct parts by time 36, and then, at time 86 after reflecting off the walls, returns to particle 2’s position. We also notice in both these figures, that at time 40 and thereafter, particle 2 (our “barrier”) fissions and there are two peaks in the x_2 dependence.

As this comparison of Figures 2 and 3 demonstrates, it seems easier to understand the

m–m, Repulsive Vsquare

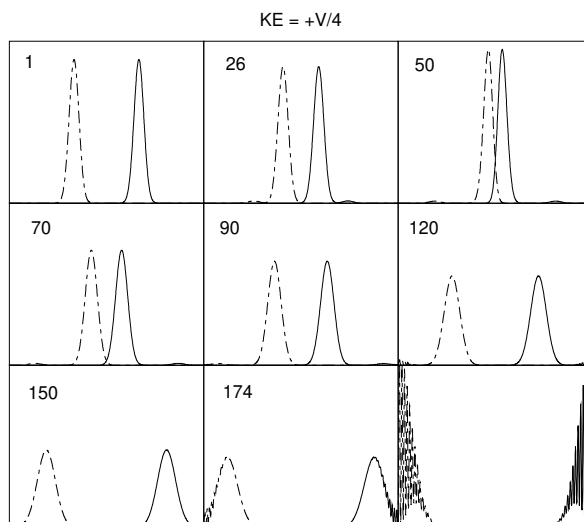


Figure 5: Same as Fig. 4, except now for a repulsive m – m collision in which the mean energy equals one quarter of the barrier’s height.

physics by superimposing two single-particle densities (thereby discarding information on correlations) than by examining the two-particle density. Accordingly, the figures we show hence, and the majority of the animations on the Web, are of single-particle densities.

Fig. 3 is similar to the behavior present in Schiff’s one-particle simulation, Fig. 1, but without ripples during the collision. Those ripples are caused by interference between scattered and incident wave, and even though we have a square barrier potential acting between the particles, neither particle “feels” the discontinuity of the sharp potential edge at any one time. However, there are ripples when our wavepackets hit the walls, as seen at times 55 and 150. (There is also a ripple at time 36 arising from interference with the small, reflected part of the left edge of 1’s initial wavepacket. This artifact of having particle 1 so near the left edge of the bounding box can be seen reflecting off the left wall at time 18.)

Something new in Fig. 3, that is not in Schiff, is the delayed “fission” of the heavier particle’s wavepacket after time 40 due to repulsion from the reflected and transmitted parts of wavepacket 1. In addition, at time 86 we see that the reflected and transmitted parts of 1 have reconstituted themselves into a single but broadened wavepacket, that at time 150 is again being reflected from the left wall.

In Fig. 4 we see another m – $10m$ collision. This time there is an attractive interaction between the particles and again the mean energy equals half the well depth. Even though the kinetic energy is low, the interaction is attractive and so particle 1 passes through particle 2. However, some of wavepacket 1 is reflected back to the left after the collision, and, as we see at time 55, the wavepacket for the heavy particle 2 fissions as a consequence of its attraction to the two parts of wavepacket 1.

Although we do not show them here, on the Web we also display movies of collisions corresponding to a Gaussian potential acting between the particles. These are much softer collisions and have behaviors similar to classical particles bouncing off each other, with squeezing and broadening of the wavepackets, but little breakup or capture.

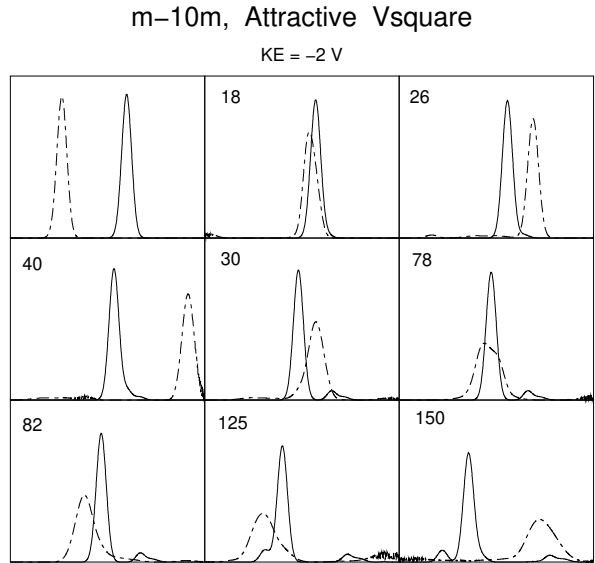


Figure 6: Same as Fig. 4, except now for an attractive m - m collision in which the mean energy equals one quarter of the well's depth.

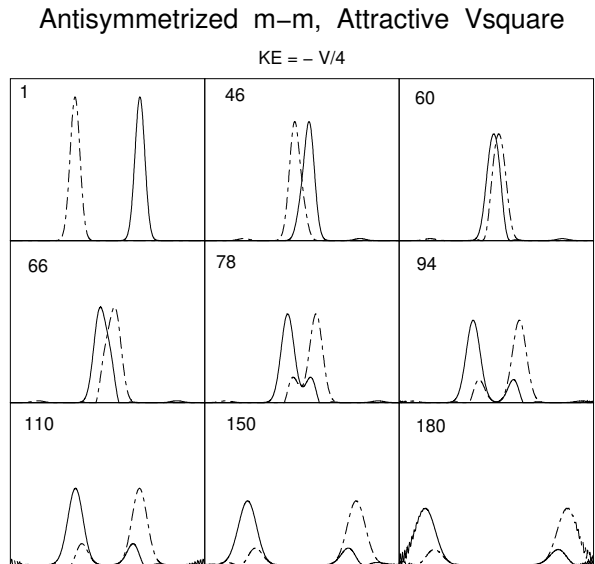


Figure 7: Same as Fig. 4, except now for an attractive m - m collision in which the mean energy equals one quarter of the well's depth, and for which the wavefunction has been antisymmetrized.

Symmetrized m - m , Attractive V square

$$KE = -V/4$$

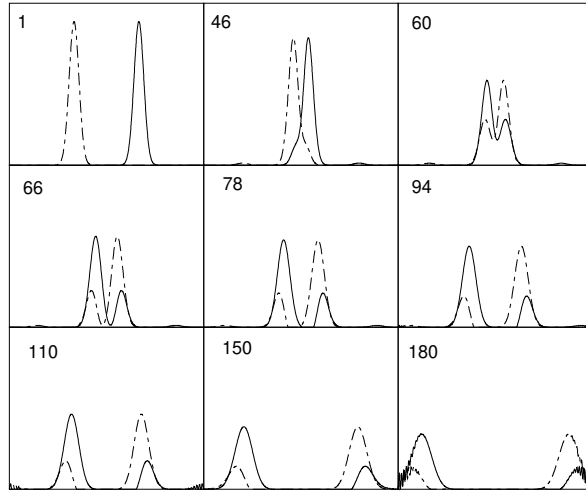


Figure 8: Same as Fig. 4, except now for an attractive m - m collision in which the mean energy equals one quarter of the depth, and for which the wavefunction has been symmetrized.

4.3 m - m Collisions

In Fig. 5 we show nine frames from the movie of a repulsive m - m collision in which the mean kinetic energy equals one quarter of the barrier height. The initial packets are seen to slow down as they approach each other, with their mutual repulsion narrowing and raising the packets up until the time (50) when they begin to bounce back. The wavepackets at still later times are seen to retain their shape, with a progressive broadening until they collide with the walls and break up. As shown on the Web, when the mean energy is raised there will be both transmitted and reflected wave, already seen in Fig. 3 for an m - $10m$ collision.

In Fig. 6 we show nine frames from the movie of an attractive m - m collision in which the mean energy equals one quarter of the well depth. The initial packets now speed up as they approach each other, and at time 60 the centers have already passed through each other. After that, a transmitted and reflected wave for each packet is seen to develop (times 66-78). Finally, each packet appears to capture or “pickup” a part of the other packet and move off with it (times 110-180).

In Fig. 7 we repeat the collision of Fig. 6, only now for a wave function that has been *antisymmetrized* according to (7). The antisymmetrization is seen to introduce an effective repulsion into what is otherwise an attraction (compare the two figures for times 60-66). Again, some capture of the other wavepacket is noted from times 94 on, only now the internal captured wavepacket retains its Gaussian-like shape, apparently the result of decreased interference.

Finally, in Fig. 7 we repeat the collisions of Figures 6 and 7, only now for a wave function that has been *symmetrized* according to (7). The symmetrization is seen to introduce an effective added attraction (compare the three figures for time 60 which shows the greatest penetration for the symmetrized case). While there is still capture of the other wavepacket, the movie gives the clear impression that the wavepackets interchange with each other as a

consequence of the symmetrization.

5 Summary and Conclusions

We have assembled and tested a general technique for the numerical solution of the two-particle, time-dependent Schrödinger equation. Because the technique is general, application to two or three dimensions and for other potentials and initial conditions should be straightforward. For example, further studies may want to investigate initial conditions corresponding to bound particles interacting with a surface, or the formation of a molecule near a surface.

The Goldberg-Schiff's image (Fig. 1) of a wavepacket interacting with a potential barrier is still a valuable model for understanding the physics occurring during a particle's collision. Here we have extended the level of realism to what a collision between two particles looks like. In doing so with a simple square-well potential between the two particles, we have discovered that fission and particle pickup occur quite often, although the physics may be quite different from that in nuclei. While somewhat of a challenge to understand fully, we have also provided animations of the behavior of the two-particle density during collisions. We have placed the animations, source codes, and movie-making instructions on the Web with the hope that future students will also carry some of these images of the quantum world with them.

6 Acknowledgments

We wish to thank an anonymous referee, Henri Jansen, Al Stetz, Al Wasserman, and Roy Schult for helpful and illuminating discussions. Support has been provided by the U.S. National Science Foundation through the Northwest Alliance for Computational Science (NACSE) and the REU program, and the U.S. Department of Energy Office of High Energy and Nuclear Physics. RHL wishes to thank the San Diego Supercomputer Center and the Institute for Nonlinear Science at UCSD for their hospitality.

References

- [1] L.I. Schiff, *Quantum Mechanics* (third edition), McGraw-Hill, New York (1968), p 106.
- [2] A. Goldberg, H. M. Schey, and J. L. Schwartz, *Computer-Generated Motion Pictures of One-Dimensional Quantum-Mechanical Transmission and Reflection Phenomena*, *Amer. J. Phys.*, **35**, 177–186 (1967).
- [3] S.E. Koonin, *Computational Physics*, Benjamin, Menlo Park, 176–178 (1986).
- [4] N.J. Giordano, *Computational Physics*, Prentice Hall, Upper Saddle River, 280–299 (1997).
- [5] R.H. Landau and M.J. Paez, *Computational Physics, Problem Solving With Computers*, Wiley, New York, 399–408 (1997).
- [6] S. Brandt and H.D. Dahmen, *Quantum Mechanics on the Personal Computer*, Chapt. 5, Springer-Verlag, Berlin, 82–92 (1990).

- [7] A. Askar and A.S. Cakmak, *Explicit Integration Method for the Time-Dependent Schrödinger Equation for Collision Problems*, J. Chem. Phys., **68**, 2794–2798 (1978).
- [8] P.B. Visscher, *A Fast Explicit Algorithm for the Time-Dependent Schrödinger Equation*, Computers In Physics, 596–598 (Nov/Dec 1991).
- [9] *Movies of Wavepacket–Wavepacket Quantum Scattering*,
[href://nacphy.physics.orst.edu/ComPhys/PACKETS/](http://nacphy.physics.orst.edu/ComPhys/PACKETS/)
- [10] Our animations are animated *gifs* that can be viewed with any Web browser, or viewed and controlled with a movie player such as *Quick Time*. To create them, we have the C code *packets.c* output files of wavefunction data for each time. We plot each data file with the Unix program *gnuplot* to produce one frame, and then convert the plots to gif files. We then use *gifmerge* [12] to merge the frames into an animation. Further information and instructions for making movies using different operating systems and formats can be found on the Landau Research Group Web pages[9, 11].
- [11] *Visualization Of Scientific Data*, <http://nacphy.physics.orst.edu/DATAVIS/datavis.html>
- [12] GIFMerge Rev 1.30 (C) 1991,1992 by Mark Podlipec, improvements by Rene K. Mueller 1996; see too <http://www.iis.ee.ethz.ch/~kiwi/gifmerge.html>.